Rotational Dynamics of Naphthalene-Labeled Cross-link Junctions in Poly(dimethylsiloxane) Elastomers

ARTICLE *in* THE JOURNAL OF PHYSICAL CHEMISTRY · MAY 1996

Impact Factor: 2.78 · DOI: 10.1021/jp953632u

4 AUTHORS, INCLUDING:

Andrew H Marcus
University of Oregon
81 PUBLICATIONS **1,404** CITATIONS
SEE PROFILE

Curtis W. Frank
Stanford University
363 PUBLICATIONS **9,974** CITATIONS
SEE PROFILE

Rotational Dynamics of Naphthalene-Labeled Cross-link Junctions in Poly(dimethylsiloxane) Elastomers

Pieter B. Leezenberg,[†] A. H. Marcus,[‡] Curtis W. Frank,[§] and M. D. Fayer*[,‡]

Departments of Materials Science and Engineering, Chemistry, and Chemical Engineering, Stanford University, Stanford, California 94305-5025

Received: December 7, 1995[⊗]

A series of end-linked poly(dimethylsiloxane) (PDMS) networks were prepared with different cross-link functionalities and molecular weights. This was achieved by simultaneous end-linking and self-condensation of a trifunctional silane cross-link precursor. These networks had a nonpolar naphthalene chromophore covalently attached to a fraction of the cross-link junctions. We probe the time-dependent reorientation of the naphthalene, and infer reorientation of the cross-links, by determining the time-dependence of the fluorescence depolarization in the picosecond time domain. A two-step relaxation model describes the orientational dynamics. Fast, partial depolarization in a restricted geometry is superimposed on a slower relaxation that completely depolarizes the fluorescence. We determine the two rotational diffusion constants at temperatures varying from 235 to 298 K, while we vary network parameters such as cross-link density, molecular weight, and macroscopic strain. These diffusion constants have an Arrhenius activation energy of 11.4 ± 0.8 kJ/mol. The fast relaxation is driven by motions of a few chain segments; this process is dominated by the density of the network polymer around the labeled cross-links. The slower, complete reorientation is driven by cooperative motions of a larger number of chain segments connected to the cross-link that are insensitive to steric constraints in the immediate vicinity of the cross-links.

I. Introduction

Model networks of known molecular weight between cross-links, M_c, and cross-link functionality, ϕ, are used to test molecular theories of rubber elasticity. These networks can be prepared by end-linking telechelic polymers using a ϕ-functional cross-linking precursor. For this study, we prepared PDMS elastomers through the condensation reaction of hydroxy-terminated PDMS with hydrolyzed trifunctional alkoxysilanes. In the presence of water and a catalyst this reaction is not quantitative, since the hydrolyzed alkoxysilanes will react with each other in a self-condensation reaction, forming silane clusters with an effective average functionality $\phi_{avg} > \phi$, resulting in an elastically active cross-link density, μ_a. The relative rates of the end-linking and homopolymerization reactions will determine the size and functionality distribution of the cross-link junctions and other network structure parameters. By manipulation of the stoichiometry, the resulting PDMS network structure and, hence, the mechanical, transport, and swelling properties can be controlled. We determine the swelling behavior of the various PDMS networks and use swelling theory to make assumptions about the network structure.

Chain segments and cross-link junctions in rubber networks above T_g (∼−125 °C) are subject to random Brownian motion. These network motions occur on a range of time and distance scales.[1−5] As a result, the motion of the cross-links is also heterogeneous in nature and has to be described by a distribution of relaxation times. Various rubber elasticity theories make contrasting assumptions about motions of the cross-links, and the predicted network modulus varies wth the motional freedom of the cross-links.

The dynamical behavior of cross-link junctions is dependent on the network structure. In previous work,[6,7] cross-link motions in PDMS networks were studied through the time-dependent decay of fluorescence anisotropy of the polar dansyl chromophore bound to the cross-link junctions through a propyl spacer molecule. In this study we determine the decay of fluorescence anisotropy from nonpolar 2-naphthalene that is directly bound to the cross-link junctions. We incorporate this probe into the network by having naphthyltriethoxysilane (NTES) participate as a cross-linking precursor in the network-forming reaction.

The aim of this study is to correlate the structure of the network to the local rotational motions, as probed by time-dependent fluorescence depolarization. In particular, we monitor the change of probe rotational dynamics as a function of the network chain length, M_c, and cross-link functionality, ϕ_{avg}. We also determine the influence of macroscopic strain on the cross-link rotational dynamics by monitoring the fluorescence depolarization when the network is swollen in a low viscosity oil. For networks with these varying parameters, we determine $r(t)$, the time-dependent fluorescence anisotropy. Subsequently using the fitting parameters in a model that describes rotational diffusion, we determine the rotational diffusion constants.

II. Experimental Methods and Procedures

A. Sample Preparation. Network Preparation. Hydroxyl-terminated PDMS, methyltriethoxysilane (MTES), and tin octoate catalyst were obtained from Hüls-Petrarch and were used without further purification.

We determined the number average molecular weight of the three different PDMS network precursors by GPC, using linear PDMS from the American Polymer Corp. as standards and toluene as the solvent. We found the following molecular

[†] Department of Materials Science and Engineering.
[‡] Department of Chemistry.
[§] Department of Chemical Engineering.
[⊗] Abstract published in *Advance ACS Abstracts,* April 15, 1996.

S0022-3654(95)03632-X CCC: $12.00

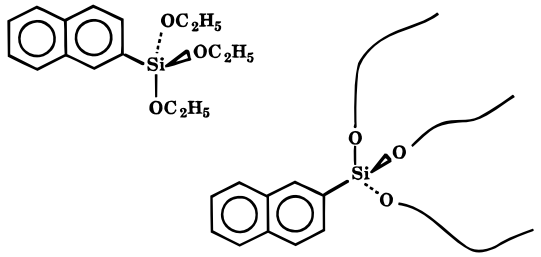

Figure 1. Probe molecule naphthyltriethoxysilane (NTES), free and bound to a trifunctional cross-link junction.

weights and polydispersities:

viscosity (cs)	M_n	polydispersity
100	4 300	1.67
750	15 200	1.88
3500	28 600	2.19

The PDMS was end-linked at room temperature by using a mixture of trifunctional ethoxysilanes with varying stoichiometric ratio r. We define r as the number of ethoxy groups per silanol chain end.

A cross-linker mixture was prepared containing 99.9 mol % MTES and 0.1 mol % naphthyltriethoxysilane (NTES), diluted in 40 vol % tetrahydrofuran (THF). This mixture was pipetted and stirred into the PDMS. Then 1 wt % catalyst (catalyst dissolved in 50% methyl-terminated PDMS) was added and stirred for 3 min. Polyethylene embedding molds were filled with 2.5 mL of the uncured mixture. These samples were cured at room temperature under nitrogen for 48 h at a relative humidity of 15%, followed by 72 h under vacuum. The samples were then swollen in THF for 62 h to extract all unreacted materials. Next, increasing amounts of methanol were added to deswell the samples. Samples were weighed prior to and after extraction to determine the sol fraction. All weighing was done on a Mettler A240 microbalance with an accuracy of 10^{-4} g.

We cut the samples to obtain a thickness that would result in an optical density between 0.02 and 0.1 at $\lambda_{exc} = 320$ nm.

Preparation of the Fluorescent Probe. Magnesium and 2-bromonaphthalene were both purchased from Lancaster. The magnesium was heated under nitrogen with a heatgun prior to the reaction. Tetraethylorthosilicate (TEOS) was purchased from Fisher Scientific and was vacuum distilled prior to the reaction. Aldrich reagent grade diethyl ether was dried over $LiAlH_4$ prior to use.

NTES was prepared by means of a Grignard reaction. The Grignard reagent was prepared by reacting 12.0 g of 2-bromonaphthalene with 1.76 g of magnesium shavings in diethyl ether, using an ultrasonic bath at 50 ± 10 °C. This reagent was transferred dropwise into 150 g of TEOS. We used approximately a 10-fold excess of TEOS to minimize the number of dinaphthyl-substituted silanes. We let this mixture react under a nitrogen atmosphere for 72 h at its boiling point of 35 ± 2 °C. The mixture was gently refluxed using a heating mantle. After 72 h, the reacted mixture was filtered and rotoevaporated, and the product was partitioned by fractional distillation at 275 °C. We recorded NMR and GC-MS spectra as described elsewhere,[8] to determine that the NTES product was at least 98% pure. We obtained the NMR spectrum from NTES in chloroform after purification. In Figure 1 we show the NTES probe free and bound to a trifunctional cross-link junction.

Dispersion of the Chromophore. We prepared unlabeled networks according to the same protocol as described above, but without NTES in the cross-linker mixture. We dispersed NTES inside unlabeled networks in the following way. First, we prepared a 10^{-4} M solution of NTES in 95 vol% methanol/5 vol% THF. We swelled unlabeled networks for 24 hours in this swelling mixture. After this we dried the networks for 48 h in air and for 24 h in vacuum. As a result we obtained networks with free NTES mixed in. The optical density of these samples at 320 nm was 0.2.

B. Characterization. Time-dependent decay of fluorescence anisotropy was measured by using the time-correlated single photon counting technique. The frequency doubled output of a Spectra Physics mode-locked, Nd:YAG laser was used to synchronously pump a dye laser. The dye laser was cavity dumped with a Bragg cell to produce a single pulse at 640 nm that was frequency doubled to give the excitation pulse. The excitation pulse energy was typically 1 nJ, with a bandwidth of 0.5 nm. The excitation pulse typically had a duration of 10 ps at 320 nm.

The polarization of the excitation pulse was rotated with a Pockels cell, while the detector polarizer was kept at vertical polarization. This eliminated errors due to varying efficiency of the detection system as a function of polarization. Front face fluorescence was focused into a monochromator tuned to 340 nm with a polarizer at the entrance slit. A Hamamatsu R1645U-01 microchannel plate detector was used to detect the fluorescence. The instrument response at 320 nm was a Gaussian curve with a typical half-width of 50 ps. The system has been described in more detail elsewhere.[9,10]

We checked for birefringence by placing a polarizer and a phototube in the excitation beam path after letting it pass through the sample. The ratio of transmitted light parallel and perpendicular to the incident polarization was measured. This ratio was 150:1 or higher, indicating that there is no distortion of the data due to birefringence.

A sample containing randomly oriented chromophores is excited by the plane polarized light pulse of 10-ps duration. Chromophore motion leads to rotation of the transition dipole relative to the excitation polarization and thus depolarizes the emitted light. We excited the naphthalene moieties with polarized light at $\lambda_{exc} = 320$ nm and determined the time-dependent decay of the fluorescence intensity at $\lambda_{em} = 340$ nm. We measured both I_{par}, the intensity of the fluorescence parallel to the excitation polarization, and I_{perp}, the intensity perpendicular to it. From these two signals, we calculate the fluorescence anisotropy $r(t)$ at each time point:

$$r(t) = \frac{I_{par}(t) - I_{perp}(t)}{I_{par}(t) + 2I_{perp}(t)} \tag{1}$$

The time-dependent intensities $I_{par}(t)$ and $I_{perp}(t)$ can be written as

$$I_{par}(t) = e^{-t/\tau}(1 + 2r(t))$$

$$I_{perp}(t) = e^{-t/\tau}(1 - r(t)) \tag{2}$$

where τ is the fluorescence lifetime. Substitution of these equations into eq 1 shows that $r(t)$ is independent both of the fluorescence lifetime τ and of the functional form of the population decay.

The maximum number of counts per second varied from 10 000, in samples with OD = 0.2, down to 2000 in some samples with a lower optical density. The spot size of the excitation pulse was approximately 1 mm in diameter. We collected four data sets (I_{par} and I_{perp}) at each temperature to improve the signal to noise ratio. For fitting, we averaged these four $r(t)$ curves.

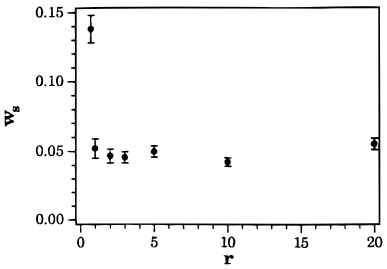

Figure 2. Weight fraction of soluble material w_s as a function of stoichiometric ratio r.

TABLE 1: v_{2m}, Volume Fraction of Polymer Inside Networks Swollen to Equilibrium in Toluene, for Networks Prepared with Different Excess Ratio r

r	v_{2m}	r	v_{2m}
0.7	0.116	5.0	0.277
1.0	0.187	10	0.296
2.0	0.245	20	0.307
3.0	0.260		

After plotting the natural log of ($I_{par} + 2I_{perp}$) as a function of time, we determined from the slope of this plot that the naphthalene fluorescence lifetime was 45 ns. This lifetime was independent of the cross-link size, the molecular weight of the polymer, and the temperature.

The value of $r(t=0)$ that we found in all of our measurements was 0.2. This $r(t=0)$ value is below the maximum value of 0.4 for a perfectly polarized transition. It has been argued that the detection of broad band fluorescence of NTES can result in reduction of the transition polarization.[8] The experimental variable is the time dependence of the anisotropy decay. In contrast to a steady state fluorescence depolarization experiment, the information is available even though $r(t=0)$ is observed to be less than 0.4. The $r(t=0) = 0.2$ value is the same as found for 2-substituted naphthalenes in other fluorescence depolarization experiments, where excellent agreement between experiment and theory was found.[9−11]

The sample was held at low temperatures using a liquid helium closed cycle refrigerator. This gave a temperature stability of ±0.5°.

Steady state fluorescence spectra were measured with a Spex Fluorolog 212 spectrometer. The light source was a 450-W xenon lamp. We used slit widths of 2 mm, corresponding to a spectral band width of 5 nm. All spectra were measured against a reference solution of Rhodamine-B in propylene glycol and were corrected for the instrument response.

III. Results

A. Characterization of the Network Structure. We prepared elastomeric networks with stoichiometric ratio, r, varying from 0.7 to an excess of 20 ethoxy groups per chain end. In Figure 2, we show the extractable or sol fraction w_s of the reactants that we find from our networks prepared with different r. Most of the mass of the sol fraction is made up of unreacted polymer chains. Therefore, Figure 2 shows that the amount of reactive polymer that is incorporated into the network is approximately independent of r, for all $r > 0.7$.

To characterize these networks, we let them swell to equilibrium in toluene and determined v_{2m}, the volume fraction of polymer in the swollen networks. In Table 1, we show v_{2m} for the networks prepared with different stoichiometric ratio r.

According to rubber elasticity theories, swelling behavior of model networks can be related to the cycle rank ξ, a parameter that uniquely describes the network structure. We will use the phantom model here to derive ξ, since it has been shown to be fairly accurate for elastomers that are swollen to a large extent.[12−14] In swelling equilibrium, the cycle rank of a network prepared in the dry state can be calculated according to[12−14]

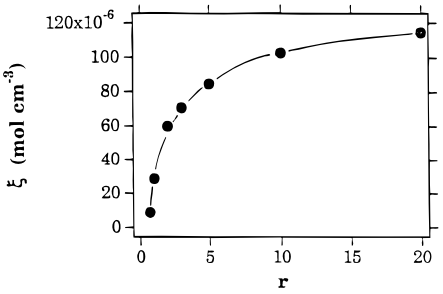

Figure 3. Cycle rank ξ as a function of stoichiometric ratio r, calculated from v_{2m} found for PDMS elastomers swollen to equilibrium in toluene.

$$\xi = \frac{[\ln(1 - v_{2m}) + \chi v_{2m}^2 + v_{2m}]}{-V_1 v_{2m}^{1/3}} \tag{3}$$

where V_1 is the molar volume of the solvent (107 cm^3 mol^{-1} for toluene at 25 °C) and χ is the interaction parameter between solvent and polymer. The interaction parameter χ depends on the polymer volume fraction v_2; we use a literature value

$$\chi = 0.445 + 0.297 v_2 \tag{4}$$

which was obtained from light scattering measurements of linear PDMS in toluene solution.[15] In Figure 3, we plot ξ as a function of r, for r varying from 0.7 to 20. At low r we find the strongest dependence of ξ on r.

The cycle rank of a network is the number of chains that have to be cut in order to obtain a giant acyclic molecule.[13,16,17] The structure parameter ξ is related to ν_a and μ_a by

$$\xi = \nu_a - \mu_a \tag{5}$$

where ν_a is the concentration of elastically active chains that are connected to active cross-links at both ends, and μ_a is the concentration of elastically active cross-links that are connected to the network through three or more branches. Model networks that are prepared with a ϕ-functional cross-linking precursor that only reacts with chain ends will result in a ϕ-functional network structure. In our system, the homopolymerization of the silane cross-linking precursor occurs simultaneously with the end-linking reaction. A distribution of cross-link sizes and effective functionalities results.

For our networks containing a finite amount of imperfections,

$$\mu_a = \frac{2}{\phi_{avg}} \nu_a \tag{6}$$

where ϕ_{avg} is the average number of chains connected to the infinite network per junction. Thus

$$\xi = \left(1 - \frac{2}{\phi_{avg}}\right) \nu_a \tag{7}$$

This expression for ξ characterizes the network structure. We obtained the cycle rank ξ experimentally using eq 3. However, eq 7 contains two unknown structure parameters, ϕ_{avg} and ν_a. For determination of ϕ_{avg}, we need an independent estimate of ν_a.

Elsewhere we describe the network forming reaction in a combined kinetic and statistical model,[18] based on work by Miller and Macosko.[19] In this model, w_s, the experimentally observed weight fraction of extractable, unreacted starting

material, can be used to estimate the relative rates of the competing reactions and, hence, ϕ_{avg} and ν_a. Since the exact proportionality between r and ϕ_{avg} remains unknown, we will in the following sections use the stoichiometric ratio r to indicate the network structure of a given sample.

From Figure 2 we find that the amount of polymer in the networks is independent of r for $r > 0.7$. Simultaneously, ξ, and thus the difference $(\nu_a - \mu_a)$ increases with r, as seen in Figure 3. According to eq 5, this means either that more chains are elastically active or that the effective functionality goes up, or both. These simultaneous trends show that the effective functionality ϕ_{avg} increases with r for $r > 0.7$.

The formation of network structures that we observe with r as high as 20 indicates a significant degree of silane self-condensation. According to statistical theory, in the absence of silane self-condensation, end-linking with large excess ratio of silane cross-linking moieties ($r \gg 1$) does not result in a network.[15,20] If the reaction would go to completion without self-condensation, the majority of the chain molecules would be end-capped with a silane that is not bound to at least two other chains, which is required to establish an elastically active junction.

Alkoxysilane self-condensation has received little attention in previous work on rubber elasticity that employs this type of curing chemistry. Experimental studies of high functionality PDMS networks have in general employed the reactive Si−H groups in hydromethylsiloxanes to end-link vinyl-terminated PDMS chains;[12,17,21−23] in this system no self-condensation occurs. Figures 2 and 3 give quantitative evidence of significant self-condensation of the silanes during the network-forming reaction. This reaction results in a ϕ_{avg} in the networks larger than the ϕ of the cross-link precursor.

B. Absence of Chromophore Aggregation. At high naphthalene concentrations there is a possibility of fluorescence anisotropy decay due to excitation energy transfer (EET),[9,10] since naphthalene is both an excitation energy donor as well as an acceptor with a Förster radius of 12.6 Å. This would be convoluted with anisotropy decay due to probe reorientation. We want to avoid EET, and therefore we need to maintain a reduced chromophore density $\rho_{red} < 1$. The quantity ρ_{red} is the number of naphthalenes present in the volume swept out by the Förster radius of any naphthalene. We have calculated ρ_{red} for all the samples, for the hypothetical situation where the probes are all incorporated in the network and are perfectly dispersed throughout the sample volume. The values of ρ_{red} vary between 0.0005 (for $M_n = 28\,600$ and $r = 0.7$) and 0.0258 (for $M_n = 15\,200$ and $r = 20$). For these values, EET will not be significant.

At low ρ_{red}, fluorescence depolarization due to EET may still occur if the probes are aggregated. There is no aggregation of the nonpolar naphthalene moieties in the PMDS oil prior to cure,[8] and hence we do not expect to find these probes clustered on the same cross-link junction. Below T_g of the network, probe rotation due to Brownian motion of the labeled cross-links is frozen out. In the absence of EET, there should be no decay of $r(t)$ below $r(t=0)$. We measured $r(t)$ when a sample prepared with $r = 20$, $M_n = 15{,}200$ was quenched to $T = 78$ K, and we observed that $r(t) = 0.2$, independent of time. This indicates that the chromophores do not aggregate at the cross-links.

Another sign of possible aggregation of the probes might be the formation of excimers.[11] We obtained the steady fluorescence spectra for all samples at $T = 298$ K, excited at $\lambda_{exc} = 320$ nm. The spectra coincide with the monomer spectrum obtained under the same conditions from 10^{-5} M NTES dissolved in THF. There are no low energy bands indicative of excimer formation in these spectra, giving additional evidence of absence of probe aggregation.

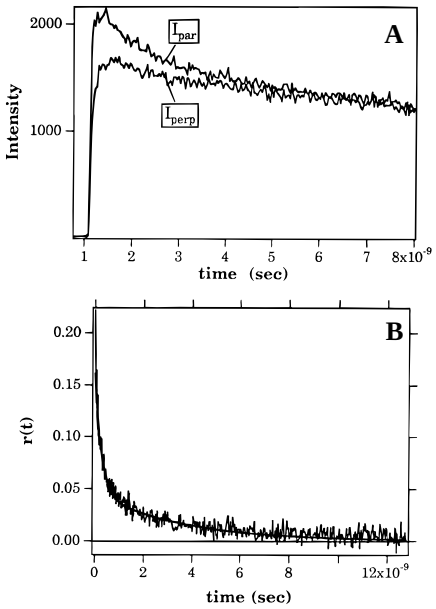

Figure 4. (**A**) I_{par}, the intensity of the fluorescence parallel to the excitation polarization, and I_{perp}, the intensity perpendicular to it, as a function of time at $T = 235$ K, for networks prepared with $r = 3$ and $M_n = 15\,200$. (**B**) Fluorescence anisotropy as a function of time at $T = 235$ K and best-fit biexponential decay curve.

The above observations show that in the temperature range between 235 and 298 K, the fluorescence anisotropy decays as a result of rotation of the chromophores and not due to EET or excimer formation.

C. Time-Dependent Fluorescence Depolarization. Above the PDMS melting temperature ($T_m \approx 190$ K[18]), the rubber network is in the amorphous state and the polymer backbone undergoes random Brownian motion. As a result of this Brownian motion, the cross-link junctions will both translate and rotate. A naphthalene that is covalently bound directly to the cross-link junction will move accordingly. We can use the time-correlated single photon technique to measure the time dependence of the rotational part of this motion.

We measured the decay of both I_{par} and I_{perp}. In Figure 4A, we plot these two intensities for the sample prepared with $r = 3.0$ and $M_c = 15\,200$, after averaging.

In Figure 4B we plot $r(t)$, the fluorescence anisotropy as a function of time at 235 K obtained from the intensities shown in Figure 4A. $r(t)$ was calculated according to eq 1. We fitted this decay of $r(t)$ to a number of different functional forms. Fitting the decay data with a biexponential function[24] gave excellent fits and low χ^2. These functions are of the following form:

$$r(t) = \sum_i A_i \exp\left(-\frac{t}{\tau_i}\right) \tag{8}$$

where A_i is a preexponential constant and τ_i is a relaxation time constant. We show the biexponential fit in Figure 4B; for this sample, we found the relaxation constants $\tau_1 = 3.67 \times 10^{-10}$ s and $\tau_2 = 4.62 \times 10^{-9}$ s. Fitting $r(t)$ to a stretched exponential did not result in acceptable fits.

D. Two-Step Relaxation Dynamics. The characteristic relaxation time of the fluorescence anisotropy decay gives information about the rate of reorientation of the probe due to Brownian motions. For rotation of a completely asymmetric chromophore, in principle five exponentials appear in $r(t)$.[24]

When the transition dipole moment is parallel or almost parallel with one of the axes of the moment of inertia tensor, the decay reduces to two exponentials. If the rotation of a spherical probe is unrestricted, i.e., if it is free to sample all orientations, then the rotational diffusion constant D is related to a single rotational relaxation time τ through:

$$D = \frac{1}{6\tau} \tag{9}$$

However, interpretation of our $r(t)$ data in terms of unrestricted rotational dynamics was not consistent with the data. The two decay constants consistently showed a different temperature dependence in various samples. If the biexponential decays arose from the unrestricted orientational relaxation, the two components should show the same temperature dependence, determined by the temperature dependence of the viscosity. For probes in a number of macromolecular,[25,26] membrane,[27] and micelle[28] systems, the observed time dependence has been explained by using a two-step model, with a fast and a slow orientational relaxation superimposed.[25] We have analyzed our $r(t)$ data within this framework, to obtain a picture of the rotational diffusion of the probes.

The initial relaxation is a restricted probe motion on a small time scale. This motion does not completely randomize the orientation. It has been referred to as wobbling within a cone. Superimposed is a slower, unrestricted motion, that can result in complete reorientation. The total correlation function $C_T(t)$ is the product of the slow and the fast correlation functions, which can be expressed as a sum:

$$C_T(t) = C_{fast}(t)C_{slow}(t)$$

$$= (1 - S^2)\exp\left(-\frac{t}{\tau_{fast}}\right) + S^2\exp\left(-\frac{t}{\tau_{slow}}\right) \tag{10}$$

where S is an order parameter, a measure of the spatial restriction of the fast motion. S gives information about the packing in the vicinity of the probe. In general, $0 \le S^2 \le 1$. If the fast motion is completely free (complete orientational relaxation), $|S| = 0$, and if the motion is completely restricted (no randomization), $|S| = 1$. We set $(1 - S^2) = A_1$ and $S^2 = A_2$, the preexponential factors from the biexponential fits.

In addition, we determine an effective correlation time τ_e, which is defined as

$$\frac{1}{\tau_e} = \frac{1}{\tau_{fast}} - \frac{1}{\tau_{slow}} \tag{11}$$

This effective correlation time is a measure of the relaxation of the local structure. We calculate τ_e from our experimental observations such as in Figure 4B, taking $\tau_{fast} = \tau_1$ and $\tau_{slow} = \tau_2$, the relaxation time constants found from the biexponential fits. S and τ_e are the fundamental parameters in the two-step relaxation model.[29]

The probe diffuses rapidly with a diffusion constant D_w in a cone with a semiangle θ_0, in analogy to the "wobbling in a cone model".[28] The dipole vector will not relax to all possible orientations. For an elongated molecule with its transition dipole moment parallel to its long axis, the cone angle θ_0 is related to the order parameter S^2 by

$$\theta_0 = \cos^{-1}\left[\frac{1}{2}\{(1 + 8|S|)^{1/2} - 1\}\right] \tag{12}$$

The diffusion constant D_w is related to the order parameter, the effective correlation time, and the cone angle. When θ_0 is small,

$$D_w = \frac{7\theta_0^2}{24\tau_e} \tag{13}$$

D_w is the diffusion constant for fast orientational relaxation in a restricted geometry. In addition, we define D_{slow} as the diffusion constant for the slower motion that causes complete reorientation of the probe. The rotational diffusion constant for complete relaxation is obtained by using eq 9, with $\tau_{slow} = \tau_2$.

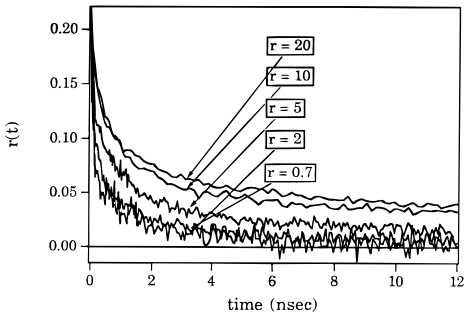

Figure 5. Fluorescence anisotropy as a function of time, at $T = 235$ K, from samples prepared with $M_n = 15\,200$ and varying stoichiometric ratio r.

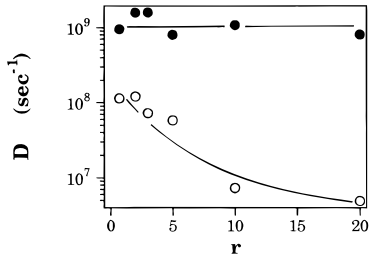

Figure 6. Diffusion constants D_w and of D_{slow} as a function of r, at $T = 298$ K, for networks prepared with $M_n = 15\,200$. ●, D_w; ○, D_{slow}.

E. Time-Dependent Reorientation of Cross-Links of Varying Size. We prepared a series of network samples with $M_n = 15\,200$ and stoichiometric ratio r, the number of ethoxy groups per silanol chain end, varying between 0.7 and 20. In Figure 5 we plot the fluorescence anisotropy decay at 298 K from this set of samples with varying r. The anisotropy decays more slowly as the excess ratio r goes up. An increase in the cross-link functionality ϕ_{avg} changes the way that the random motions of chain segments affect the ensemble averaged cross-link motion. For samples with $r > 5$, we needed a triexponential to account for an additional long-time component in $r(t)$. From the relaxation times τ_i and the preexponential factors, we then obtain D_{slow} and D_w as before, with $(1 - S^2) = A_1$, $\tau_{fast} = \tau_1$, but with $\tau_{slow} = (A_2\tau_2 + A_3\tau_3)/(A_2 + A_3)$, for use in eq 10−12. The effective correlation time is given by eq 11.

As the average cross-link size increases, the relaxation times get longer. This corresponds to slower rotational diffusion. In Figure 6 we plot the diffusion constants as a function of r at $T = 298$ K. The correlation between the diffusion constants and r is similar at each temperature. In Figure 6, the wobbling diffusion constant D_w does not change as r increases from 0.7 to 20. On the other hand, D_{slow} gets smaller as r increases from 0.7 to 20. The process of complete cross-link reorientation is slowed down as the corresponding cross-link size, ϕ_{avg}, increases. For most samples, D_{slow} is approximately an order of magnitude smaller than D_w, at any given temperature. Using eq 12, we also determined the cone angle θ_0 for our samples.

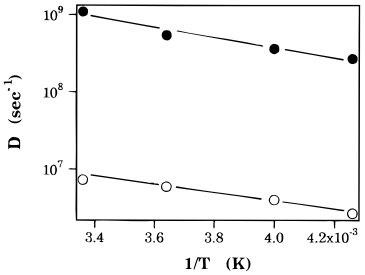

Figure 7. Diffusion constants D_w and D_{slow}, as a function of reciprocal temperature $1/T$, for networks prepared with $M_n = 15\,200$ and $r = 10$. ●, D_w; ○, D_{slow}.

TABLE 2: Arrhenius Activation Energies of the Constants D_w and D_{slow} for Restricted Rotational Diffusion of the Probe Molecules

r	$E_a(D_w)$, kJ mol^{-1}	$E_a(D_{slow})$, kJ mol^{-1}
0.7	11.2	12.2
2.0	11.5	11.9
3.0	11.9	12.5
5.0	10.9	12.4
10	11.0	10.3
20	9.6	10.8

There is no clear dependence of θ_0 on the average cross-link functionality ϕ_{avg}.

F. Temperature Dependence of Cross-Link Reorientation. We determined the time-dependence of the fluorescence anisotropy decay of all samples over a temperature range from 235 to 298 K. Below 235 K the appearance of crystallites causes scattering, which causes additional depolarization.[30] We fit the decay curves to a multiexponential function and obtained D_w, D_{slow}, and θ_0. For the sample prepared with $r = 10$, we show these diffusion constants as a function of $1/T$ in Figure 7. A linear dependence between these quantities indicates an Arrhenius relationship for the diffusion constants:

$$D = D_0 \exp\left(-\frac{E_a}{RT}\right) \tag{14}$$

where D_0 is a temperature-independent preexponential factor, E_a is an activation energy, and R is the gas constant. For the samples prepared with different excess ratio r, we always observed a linear relationship between the log of both Ds and $1/T$. By fitting these points to a least squares fit, we obtained the activation energy. We show these activation energies in Table 2: $E_a(D_w) = 11.0 \pm 0.7$ and $E_a(D_{slow}) = 11.7 \pm 0.8$ kJ/mol. We conclude that over the range of $r = 0.7$ to 20, the activation energy $E_a(D) = 11.4 \pm 0.8$ kJ/mol is the same for both diffusion constants and is independent of stoichiometry, within experimental error.

For all of these samples, θ_0, the semiangle of the cone in which wobbling occurs, is dependent on the temperature. From eq 12, we determined the cone angle θ_0 for our samples at different temperatures. As the samples get colder, the cone angle gets slightly smaller in all samples. For example, in the sample with $r = 10$, θ_0 decreases monotonically from 61° at 298 K to 57° at 235 K.

G. Molecular Weight Dependence of Depolarization. Network samples of different molecular weights between the cross-links, M_c were prepared by end-linking PDMS oils of molecular weights $M_n = 4300$, 15 200, and 28 600 with a stoichiometry $r = 1.0$. We measured the time-dependent fluorescence anisotropy at $T = 298$ K for all three samples and found the decay curves to be almost identical. We measured $r(t)$ as a function of temperature in the $M_c = 4300$ and 28 600 networks. We fit the decay data to a biexponential function and obtained the diffusion constants D_w and D_{slow} as described above. In Figure 8, D_w and D_{slow} are plotted as a function of $1/T$. Within the error, the slow diffusion constant D_{slow} is the same for both molecular weights between $T = 298$ and 235 K. For networks with this cross-link functionality and with $4300 < M_c < 28\,600$, there is no dependence of the slow rotational diffusion of the cross-link on molecular weight.

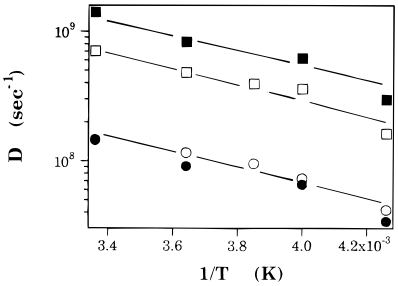

Figure 8. Diffusion constants D_w and D_{slow}, as a function of reciprocal temperature $1/T$, for networks prepared with $r = 1$, but with molecular weights $M_c = 4300$ and 28 000. ■, D_w, $M_c = 4300$; ●, D_{slow}, $M_c = 4300$; □, D_w, $M_c = 28\,600$; ○, D_{slow}, $M_c = 28\,600$.

On the other hand, D_w decreases slightly as M_c increases. The wobbling in a cone of the cross-link bound naphthalene is slowed down as the molecular weight of the matrix is increased at constant cross-link functionality. In addition, the cone angle θ_0 depends on M_c as well. At $T = 298$ K, in networks with $M_c = 28\,600$, θ_0 is 55°, whereas for $M_c = 4300$, θ_0 is 48°. In both samples θ_0 decreases by 6° when the temperature drops to 235 K.

The slopes of the curves are the same for both D_w and D_{slow} within experimental error. Therefore, the activation energies for both constants are the same and independent of M_c.

H. Cross-Link Reorientation in Swollen Networks. Applying macroscopic strain to the elastomer causes a change in the segmental mobility and orientation of the network polymer.[2,31,32] It is to be expected that the reorientational process of the cross-links will be affected by strain as well. Nonisotropic strain causes birefringence in PDMS networks, which makes interpretation of $r(t)$ data complicated. Therefore, we chose to impose strain on the network by isotropic swelling in a low viscosity solvent with an index of refraction that is the same as that of the network. The $r = 5.0$ network with $M_c = 15\,200$ was swollen to equilibrium in low viscosity, methyl-terminated siloxane oligomers (10 cs oil) at $T = 298$ K. The corresponding weight fraction of network polymer inside this swollen system $v_{2m} = 0.454$ at this temperature. This amount of isotropic swelling corresponds to a network strain of approximately 30% along each of the three sample axes.

Use of the siloxane oligomer as a swelling agent implies that the change in the chemical microenvironment of the labeled cross-links is small. Polar interactions that could possibly hinder reorientation[8] were minimized this way. We found no change in the lifetime of the probes upon swelling.

We measured $r(t)$ at $T = 235$, 250, 275, and 298 K. We subsequently fit and analyzed our data in the two-step relaxation model. In Figure 9, we plot D_w and D_{slow} as a function of $1/T$, for both the swollen and the dry network with $r = 5.0$. The fast diffusion constant D_w is identical in the dry and the swollen network. The Arrhenius activation energy for D_w, $E_a(D_w) = 10.7$ kJ/mol in the swollen network; in the corresponding dry network $E_a(D_w) = 10.9$ kJ/mol. The slow diffusion constant is smaller than in the dry network. In the swollen sample, D_{slow} is temperature independent; $E_a(D_{slow})$ is 0 kJ/mol within experimental error.

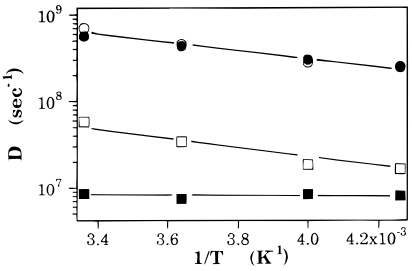

Figure 9. Diffusion constants D_w and D_{slow}, as a function of reciprocal temperature $1/T$, networks either dry or swollen in 10 cs PDMS oil; $r = 5$ and $M_n = 15\,200$. ●, D_w, swollen; ■, D_{slow}, swollen; ○, D_w, dry; □, D_{slow}, dry.

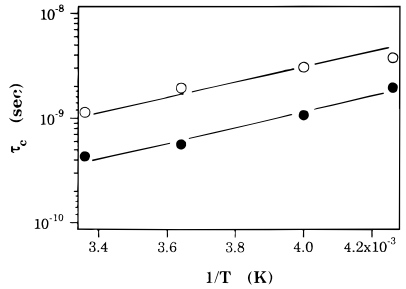

Figure 10. Correlation time constant τ_c, as a function of reciprocal temperature $1/T$, for networks prepared with $M_n = 15\,200$ and $r = 5$, with NTES either bound to the cross-link junctions or freely dispersed inside the unlabeled network. ○, dispersed NTES; ●, bound NTES.

The cone angle θ_0 in the swollen network decreases from 54° at 298 K to 44° at 235 K. In the corresponding dry network θ_0 is 55° at 298 K and 52° at 235 K.

I. Reorientation of Chromophores Dispersed in the Network. In order to compare the dynamics of this specific topological part of the network structure with the average network dynamics, we determined the rotational dynamics of the naphthalene probe when it was not covalently attached to a cross-link. For this purpose, we prepared a network sample inside of which the chromophore was dispersed in low concentrations. This network was prepared with $M_n = 15\,200$ and $r = 5.0$; 100% of the cross-link precursor moieties had methyl instead of naphthalene as the fourth substituent on the silane.

The steady state fluorescence emission spectrum excited at $\lambda_{exc} = 320$ nm showed that there were no naphthalene excimers. In analogy with the melt experiment, we assume that there is no phase separation of clustering of the NTES.[8]

We measured the fluorescence anisotropy decay of this sample at 235, 250, 275, and 298 K. We fit the decay of $r(t)$ to a biexponential function, corresponding to naphthalene rotation around two axes. From this, we determined the correlation time τ_c, which does not assume a functional relationship for the decay of $r(t)$. The correlation time is the normalized area under the decay curve. We calculated τ_c by using the constants obtained from fitting with the exponential functions:

$$\tau_c = \frac{1}{r_0}\int_0^\infty r(t)\,dt = \frac{\sum A_i\tau_i}{\sum A_i} \qquad (15)$$

In Figure 10 we plot the correlation times as a function of the inverse of temperature. In the same figure, we plot the τ_c's from a network prepared with $M_c = 15\,200$ and $r = 5.0$, which has naphthalene attached to the cross-link junctions. The two networks have similar structures and only vary in the location of the NTES. The correlation times are shorter for the bound probes. Allowing NTES to reside anywhere in the network slows down the probe reorientation relative to when the probes are bound to the cross-links.

From the slope of $\ln(\tau_c)$ vs $1/T$ plot, we find that the activation energy of the correlation time $E_a(\tau_c)$ is 10.2 kJ/mol for the freely dispersed NTES. $E_a(\tau_c)$ is 11.3 kJ/mol for the same network with NTES covalently bound.

IV. Discussion

The fluorescence anisotropy data combined with the swelling data indicate that increasing the stoichiometric ratio r simultaneously causes an increase in ϕ_{avg}, the average cross-link functionality, and a change in cross-link rotational dynamics. However, the changes in swelling behavior and in local dynamics are not strongly correlated.

No quantitative model is available to describe the rotational diffusion rate of cross-links. Previously, a qualitative mechanism has been proposed by which the orientational correlation of labeled cross-links decays.[7] It was recognized that multiple chains emanate from a junction. Each chain experiences a range of thermal motions. Forces of chain segments acting tangential to the cross-link exert a torque on it accordingly. As a result, simultaneous translational and rotational motion of the cross-link occurs. The transition dipole moment of the chromophore loses its orientation correlation depending on the tangential forces that the cross-link experiences. It was suggested that the rotational correlation time is approximately one-third of the translational correlation time.

Having the naphthalene directly attached to the cross-link junction means that the rotation of the cross-link junction itself is probed. The fluorescence anisotropy decay from NTES dissolved in PDMS oil indicates that the NTES rotates as a rigid body in the polymer environment that is locally highly mobile.[8] If rotation of the Si−C bond (the Si−naphthyl linkage) were significantly fast, $r(t)$ would not relax as for a rigid rotor. In addition, in previous work,[7] the dansyl chromophore was covalently bound to the cross-link junctions of PDMS networks through a propyl spacer molecule. $r(t)$ was determined for these networks and the decay was fit with a biexponential. Both decay constants had the same temperature dependence, which was similar to the temperature dependence of the correlated chain motions. Thus, the reorientation of the dansyl probe was governed by the motion of polymer chains rather than by rotation around the propyl spacer. The naphthalene in our probe molecule is directly attached to the cross-link junction, instead of through a propyl linkage. Therefore, the decay of $r(t)$ is indicative of rotation of the labeled cross-link junctions.

A. Dependence of Cross-Link Diffusion Constants on Cross-Link Size. Molecular theories for rubber elasticity consider the relationship between the ensemble-averaged cross-link displacement and network deformation.[12,33] These rubber elasticity theories do not yield a prediction for the rates of cross-link motions. Ensemble average cross-link fluctuations are not explicitly considered as a function of time.

On the other hand, a number of experimental studies reported measurements of translational dynamics of cross-link junctions in polymer networks through the use of ^{2}H NMR,[34,35] NMR free induction decay,[36] and neutron spin echo.[37−39] In addition, rotational dynamics of cross-link junctions have been studied with magic angle spinning NMR[40,41] and time-correlated single photon counting.[7]

Warner[5,42] derived an expression for the translational diffusion coefficient D_ϕ of a ϕ-functional cross-link. For a polymer chain obeying Rouse-like chain dynamics, the diffusion law correlates the position of a point on a chain at time t with its position at

a later time t':

$$\langle(\mathbf{R}(s, t) - \mathbf{R}(s, t'))^2\rangle = D|t - t'| \tag{16}$$

$\mathbf{R}(s, t)$ is the coordinate of a point s along the polymer chain and at the time t. D is the diffusion constant for a monomer. The diffusivity D_ϕ of a ϕ-connected monomer slows down relative to a chain monomer connected to two other segments:

$$D_\phi \rightarrow \frac{D}{\phi/2} \tag{17}$$

A qualitatively similar trend in diffusivity with number of attached chains appears to result in Monte Carlo[43] and molecular dynamics[44] simulation studies of end-linked networks.

The prediction of eq 17—that D is proportional to $2/\phi$— is valid for small-scale ($\leq$30 Å) and short-time translations.[42] The latter constraint implies that the time is too short for neighboring cross-links or entanglements to interfere and introduce additional correlations into the dynamics. This condition appears to be met as we will see in the discussion of the molecular weight dependence of D_{slow}. If Warner's prediction is valid for rotational diffusion as well, it implies that as we increase r from 0.7 to 20, we should see a monotonic decrease of D proportional to $2/\phi$. This is in qualitative agreement with the trend in D_{slow} in Figure 6.

According to Figure 6, the wobbling diffusion constant D_w that we find does not follow the prediction from eq 17. We propose the following explanation. The spatial requirements of chain-like multifunctional junctions in PDMS networks have been analyzed by Flory,[21] for a mean diameter of the PDMS chain of 6.7 Å. The chains emanating from this type of junction occupy approximately half of the space they pervade when they are randomly configured. Polymer segments that are involved in cross-link reorientation are stretched beyond their undeformed dimensions. Some conformational changes leading to cross-link reorientation are hindered. The cross-link creates local density fluctuations in the network polymer;[45−49] specifically, these steric constraints on the polymer conformation may create a void near a cross-link.[50] Locally, PDMS behaves as a low viscosity liquid, with the backbone rotating easily along the long, partly polar Si−O bond. The local microviscosity and free volume in PDMS matrix have been the subject of numerous photophysical studies.[1,6−8,51−54] A void volume in the vicinity of the cross-link allows wobbling of the naphthalene dipole. The amount of void volume associated with the labeled cross-links appears independent of the cross-link size.

We find that the Arrhenius activation energy for the diffusion constants is essentially independent of r, as shown in Table 2. The polymer motions responsible for cross-link reorientation have an r-independent activation energy. As we increase r, on average, more chains are connected to each cross-link. As ϕ_{avg} increases, reorientation requires cooperative motions of more emanating chains. Larger scale motions are required to cause rotation of the cross-link entity. This will only happen on longer time scales, but ϕ_{avg} does not have an impact on the temperature dependence of the diffusion constants. The polymer modes that cause the rotation of the cross-link junctions all require a similar activation energy of 11.4 ± 0.8 kJ/mol, independent of r. As ϕ_{avg} becomes larger, the number of attached polymer segments that need to relax increases. In the limit of extremely large ϕ_{avg}, it is possible that the activation energy for local relaxation would increase to the value for macroscopic flow, 14 kJ/mol.[8] However, in the range of cross-link size that we probe, the experimental E_a does not increase with r.

These observations provide additional evidence that the cross-link size increases with r. The Debye−Stokes−Einstein equation gives the hydrodynamic rotational relaxation time τ_r of a body rotating in a liquid medium[7,8]

$$\tau_r = \frac{V_{eff}\eta(T)}{kT} \tag{18}$$

where V_{eff} is the effective volume of the rotating body and $\eta(T)$ is the viscosity of the medium. This relation can be used qualitatively in the present context. The viscosity of the medium probably does not change with r, since the activation energy is constant. However, the rotation becomes slower, so eq 18 indicates that the volume of the rotating entity increases. Since the severe interpenetration of chains that occurs in networks of low functionality is not present to the same extent in networks of high functionality,[55] we cannot quantify the increase in effective volume.

B. Dependence of Cross-Link Diffusion on Molecular Weight. Above T_m, the random motions of polymer backbone segments that are connected to the cross-link are responsible for cross-link reorientation. Our fluorescence anisotropy decay results correspond to different trends of D_w and D_{slow} with M_c, the molecular weight of the polymer, for a sample prepared with $r = 1$. D_{slow} is the same for molecular weights $M_c = 4300$ and $M_c = 28\,000$ as shown in Figure 8. We conclude that the complete reorientation of the probe involves molecular weights less than 4300 or, correspondingly, less than 57 repeat units. This is substantially smaller than the entanglement molecular weight $M_e \approx 8000$ for PDMS,[56] which plays an important role in the relaxation behavior of the network polymer.[44]

On the other hand, D_w, the diffusion constant for wobbling in a cone, slows down as M_c increases. In addition, the smaller cone angle θ_0 observed in the higher molecular weight networks suggests that the fast localized diffusion of the naphthalene is relatively constrained. These results suggest the following picture.

A high molecular weight between cross-links (M_c) corresponds to a low cross-link density μ_a at a given cross-link functionality. The lower cross-link density causes the network polymer to have better access to the labeled cross-link. This local crowding of polymer chain segments slows down the wobbling motion. The larger scale polymer modes that are responsible for complete reorientation of the cross-link are insensitive to these highly localized constraints.

A low M_c corresponds to a high cross-link density μ_a. A relatively large fraction of polymer segments is connected to the cross-links. Since a large fraction of the polymer chains is stretched, there is a relatively high fraction of void volume. This facilitates the fast, partial reorientation of the probes.

C. Reorientation of Cross-Links in Swollen Networks. The fast diffusion constant D_w and its temperature dependence are independent of macroscopic strain, as shown in Figure 9. The chain fragments connected to the cross-links are already extended beyond their equilibrium conformation, and macroscopic stretching does not increase that effect. Macroscopic strain only affects the Brownian motion of chain segments that are not close topological neighbors of the cross-links. Analogous to the network chains, the siloxane oligomers do not fill the local low polymer density around the cross-links. The presence of siloxane oligomers inside of the network does not affect D_w through chemical interactions, either.

The polymer segments away from the cross-links, which are involved in the complete reorientation, achieve equilibrium conformation in the dry state. These polymer fragments are stretched in the swollen network and cannot cause reorientation

as fast as when they are random coils. Hence D_{slow} becomes smaller upon swelling.

D_{slow} is relatively independent of temperature compared to the dry network. This result is convoluted by the decrease of network swelling with decreasing temperature. At lower temperatures, the networks are swollen less.[12] We would expect D_{slow} to be closer to D_{slow} of the dry network.

D. Reorientation of NTES Dispersed in the Network. The fluorescence anisotropy decay of the free NTES dispersed in the cross-linked matrix demonstrates that the rotational behavior is different than when the same probe is attached to the cross-link junction. In Figure 10 we see that when the NTES is dispersed rather than bound, rotational diffusion becomes slower. There are dynamic processes that are specific to the cross-link site and its immediate environment, as opposed to other parts of the network structure. This could be due to steric constraints associated with the introduction of a cross-link site. Since excimer formation is absent in the steady state emission spectra, we assume that the NTES does not phase separate.[8] However, NTES may be preferentially located in a specific part of the network structure.

The activation energy for the correlation time τ_c, $E_a(\tau_c)$, = 10.2 kJ/mol when the NTES is dispersed in the network and $E_a(\tau_c) = 11.3$ kJ/mol when it is covalently bound to the cross-link junctions. Elsewhere,[8] the activation energy was determined for the correlation time τ_c of reorientation of NTES dispersed in PDMS oils with M_w of 28 000 and 6000. This process has an activation energy $E_a(\tau_c) = 12.2$ kJ/mol in both oils. The activation energy for macroscopic flow of these oils was found to be 14 kJ/mol.

The naphthalenes attached to a cross-link junction have close neighboring polymer segments that are extended beyond their undeformed dimensions. When naphthalene is not confined to the cross-link, it does not experience an environment of these stretched neighboring polymer segments. As a result, the packing of network polymer immediately around it may be more dense, slowing down rotation. Crowding around the dispersed probe is stronger, leading to more restricted rotation than for probes connected to the junction.

V. Concluding Remarks

We interpret our fluorescence anisotropy observations in a two-step relaxation model, characterized by a fast diffusion constant D_w for limited reorientation in a cone with semiangle θ_0 and a slow diffusion constant D_{slow}, associated with complete reorientation of the probe.

At a given temperature, increasing r and hence increasing the average cross-link size slows down D_{slow} of the bound probe substantially. The effective volume of the cross-link increases. However, the diffusion constant D_w is independent of r. We relate D_w to a constant amount of void volume adjacent to the cross-links.

The temperature dependence of the decay constants for all samples indicate Arrhenius activated rotational motion of the cross-links. The Arrhenius activation energy for the diffusion constants is independent of cross-link size and of molecular weight. Both fast and slower probe motions are caused by segmental rotations around the Si−O bonds that form the backbone of the network polymer.

The differences between D_w and D_{slow} are attributed to the distance scale of these rotations. Wobbling in a cone is driven by constrained localized motions of the bonds immediately adjacent to the probe. The slower, complete reorientation is driven by cooperative motions of a larger number of chain segments connected to the cross-link; steric constraints in the immediate vicinity of the probe have no influence on D_{slow}. However, the slower diffusion is still "local". Complete reorientation of the labeled cross-links involves molecular weights substantially smaller than the entanglement molecular weight.

Reorientation of the free NTES probe dissolved in an unlabeled network is slow, relative to the bound probe. Since the activation energy for rotation is approximately the same in both cases, we argue that the relevant polymer motions are the same but that local packing differs and is tighter around a probe that is dispersed.

Swelling the network in a low viscosity PDMS oil slows down the slow reorientation of the probe. We attribute this to decreased rotational freedom of the strained chains emanating from a labeled cross-link junction. D_w has a different dependence than D_{slow} on all of the structure parameters in these networks.

Acknowledgment. P.B.L. and C.W.F. thank Hitachi Ltd. for support of this research. A.H.M. and M.D.F. thank the Department of Energy (DE-FG03-84ER13251) for support. The Stanford Center for Materials Research is also acknowledged for additional support and equipment.

References and Notes

(1) Ediger, M. D. *Annu. Rev. Phys. Chem.* **1991**, *42*, 225.
(2) Erman, B. In *Molecular Basis of Polymer Networks*; Baumgartner, A., Picot, C. E., Eds.; Springer-Verlag: Berlin, 1989; Vol. 42; p 100.
(3) Fytas, G.; Dorfmuller, T.; Lin, Y.-H.; Chu, B. *Macromolecules* **1981**, *14*, 1088.
(4) Heinrich, G.; Vilgis, T. A. *Macromolecules* **1992**, *25*, 404.
(5) Warner, M. *J. Phys. C: Solid State Phys.* **1981**, *14*, 4985.
(6) Stein, A. D.; Hoffmann, D. A.; Marcus, A. H.; Leezenberg, P. B.; Frank, C. W.; Fayer, M. D. *J. Phys. Chem.* **1992**, *96*, 5255.
(7) Stein, A. D.; Hoffmann, D. A.; Frank, C. W.; Fayer, M. D. *J. Chem. Phys.* **1992**, *96*, 3269.
(8) Diachun, N. A.; Marcus, A. H.; Hussey, D. M.; Fayer, M. D. *J. Am. Chem. Soc.* **1994**, *116*, 1027.
(9) Peterson, K. A.; Stein, A. D.; Fayer, M. D. *Macromolecules* **1990**, *23*, 111.
(10) Stein, A. D.; Peterson, K. A.; Fayer, M. D. *J. Chem. Phys.* **1990**, *92*, 5622.
(11) Ediger, M. D.; Domingue, R. P.; Peterson, K. A.; Fayer, M. D. *Macromolecules* **1985**, *18*, 1182.
(12) Mark, J. E.; Erman, B. *Rubberlike Elasticity, a Molecular Primer*; John Wiley and Sons: New York, 1988.
(13) Queslel, J. P.; Mark, J. E. *Adv. Polym. Sci.* **1984**, *71*, 229.
(14) Erman, B. In *Crosslinking and Scission in Polymers*; Guven, O., Ed.; Kluwer Academic Publishers: Dordrecht, Netherlands, 1990; p 153.
(15) Patel, S. K.; Malone, S.; Cohen, C.; Gillmor, J. R.; Colby, R. H. *Macromolecules* **1992**, *25*, 5241.
(16) Flory, P. J. *Macromolecules* **1982**, *15*, 99.
(17) Queslel, J. P.; Mark, J. E. *Adv. Polym. Sci.* **1984**, *65*, 135.
(18) Leezenberg, P. B. Ph.D. Thesis, Stanford University, 1994.
(19) Miller, D. R.; Macosko, C. W. *Macromolecules* **1978**, *11*, 656.
(20) Miller, D. R.; Macosko, C. W. *Macromolecules* **1976**, *9*, 206.
(21) Flory, P. J.; Erman, B. *J. Polym. Sci., Polym. Phys.* **1984**, *22*, 49.
(22) Sharaf, M. A.; Mark, J. E. *Polymer* **1994**, *35*, 740.
(23) Sharaf, M. A.; Mark, J. E.; Ahmed, E. *Colloid Polym. Sci.* **1994**, *272*, 504.
(24) Tao, T. *Biopolymer* **1969**, *8*, 609.
(25) Szabo, A. *J. Chem. Phys.* **1984**, *81*, 150.
(26) Ouano, A. C.; Pecora, R. *Macromolecules* **1980**, *13*, 1173.
(27) Kinoshita, K.; Kawato, S.; Ikegami, A. *Biophys. J.* **1977**, *20*, 289.
(28) Quitevis, E. L.; Marcus, A. H.; Fayer, M. D. *J. Phys. Chem.* **1993**, *97*, 5762.
(29) Lipari, G.; Szabo, A. *J. Am. Chem. Soc.* **1982**, *104*, 4546.
(30) Teale, F. W. J. *Photochem. Photobiol.* **1969**, *10*, 363.
(31) Besbes, S.; Bobozka, L.; Monnerie, I.; Bahar, I.; Erman, B. *Polymer* **1993**, *34*, 1179.
(32) Besbes, S.; Cernalli, I.; Bobozka, L.; Monnerie, L.; Bahar, I.; Erman, B.; Herz, J. *Macromolecules* **1992**, *25*, 1949.
(33) Vilgis, T. A. In *Elastomeric Polymer Networks*; Mark, J. E., Erman, B., Eds.; Prentice-Hall: Englewood Cliffs, NJ, 1992; p 32.
(34) Brereton, M. G. *Progr. Colloid Polym. Sci.* **1992**, *90*, 90.
(35) Brereton, M. G. *Macromolecules* **1991**, *24*, 6160.

(36) Kulagina, T. P.; Litvinov, V. M.; Summanen, K. T. *J. Polym. Sci.: Part B: Polym. Phys.* **1993**, *31*, 241.

(37) Ewen, B.; Richter, D. In *Molecular Basis of Polymer Networks*; Baumgartner, A., Picot, C. E., Eds.; Springer Verlag: Berlin, 1989; Vol. 42.

(38) Ewen, B.; Richter, D. In *Elastomeric Polymer Networks*; Mark, J. E., Erman, B., Eds.; Prentice-Hall: Englewood Cliffs, NJ, 1992; p 220.

(39) Oeser, R.; Ewen, B.; Richter, D.; Farago, B. *Phys. Rev. Lett.* **1988**, *60*, 1041.

(40) Shi, J.-F.; Dickinson, L. C.; MacKnight, W. J.; Chien, J. C. W.; Zhang, C.; Liu, Y.; Chin, Y.; Jones, A. A.; Inglefield, P. T. *Macromolecules* **1993**, *26*, 1008.

(41) Shi, J.-F.; Dickinson, L. C.; MacKnight, W. J.; Chien, J. C. W. *Macromolecules* **1993**, *26*, 5908.

(42) Warner, M. The Connectivity of Polymer Networks by Neutron Scattering. Rutherford Appleton Laboratory: London, 1982.

(43) Trautenberg, H. L.; Sommer, U.; Goritz, D. *Macromol. Symp.* **1994**, *81*, 153.

(44) Duering, E. R.; Kremer, K.; Grest, G. S. *J. Chem. Phys.* **1994**, *101*, 8169.

(45) Soni, V. K.; Stein, R. S. *Macromolecules* **1990**, *23*, 5257.

(46) Mallam, S.; Horkay, F.; Hecht, A.-M.; Rennie, A. R.; Geissler, E. *Macromolecules* **1991**, *24*, 543.

(47) Mallam, S.; Hecht, A.-M.; Geissler, E. *J. Chem. Phys.* **1989**, *91*, 6447.

(48) Geissler, E.; Horkay, F.; Hecht, A. M.; Zrinyi, M. *J. Chem. Phys.* **1989**, *90*, 1924.

(49) Hecht, A.-M.; Gullermo, A.; Horkay, F.; Mallam, S.; Legrand, J. F.; Geissler, E. *Macromolecules* **1992**, *25*, 3677.

(50) Nakanishi, S.; Yuuichi, M.; Nishikawa, M.; Amano, M.; Fujiwara, S.; Jitou, M.; Itoh, H.; Kawase, M. *J. Chem. Phys.* **1994**, *100*, 3442.

(51) Chu, D. Y.; Thomas, J. K. *Macromolecules* **1990**, *23*, 2217.

(52) Bobozka, L.; Pham-Van-Cang, C.; Giordano, C.; Monnerie, L.; Vandendriessche, J.; DeSchryver, F. C.; Kontos, E. G. *Polymer* **1987**, *28*, 1876.

(53) Pham-Van-Cang, Bobozka, L.; Monnerie, L.; Vandendriessche, J.; DeSchryver, F. C. *Polymer* **1986**, *27*, 89.

(54) Pham-Van-Cang, C.; Bobozka, L.; Monnerie, L.; Clarson, S. J.; Semlyen, J. A.; Vandendriessche, J.; DeSchryver, F. C. *Polymer* **1987**, *28*, 1561.

(55) Flory, P. J. *J. Chem. Phys.* **1977**, *66*, 5720.

(56) Stepto, R. F. T. *Eur. Polym. J.* **1993**, *29*, 415.

JP953632U